Cognitive Neurodynamics (2019) 13:519–530
https://doi.org/10.1007/s11571-019-09550-z

RESEARCH ARTICLE

Computer-aided classifying and characterizing of methamphetamine use disorder using resting-state EEG

Hassan Khajehpour[1,6] · Fahimeh Mohagheghian[4] · Hamed Ekhtiari[2,3] · Bahador Makkiabadi[1,6] · Amir Homayoun Jafari[1,6] · Ehsan Eqlimi[1,6] · Mohammad Hossein Harirchian[5]

Received: 5 March 2019 / Revised: 18 July 2019 / Accepted: 1 August 2019 / Published online: 7 August 2019

Abstract

Methamphetamine (meth) is potently addictive and is closely linked to high crime rates in the world. Since meth withdrawal is very painful and difficult, most abusers relapse to abuse in traditional treatments. Therefore, developing accurate data-driven methods based on brain functional connectivity could be helpful in classifying and characterizing the neural features of meth dependence to optimize the treatments. Accordingly, in this study, computation of functional connectivity using resting-state EEG was used to classify meth dependence. Firstly, brain functional connectivity networks (FCNs) of 36 meth dependent individuals and 24 normal controls were constructed by weighted phase lag index, in six frequency bands: delta (1–4 Hz), theta (4–8 Hz), alpha (8–15 Hz), beta (15–30 Hz), gamma (30–45 Hz) and wideband (1–45 Hz).Then, significant differences in graph metrics and connectivity values of the FCNs were used to distinguish the two groups. Support vector machine classifier had the best performance with 93% accuracy, 100% sensitivity, 83% specificity and 0.94 F-score for differentiating between MDIs and NCs. The best performance yielded when selected features were the combination of connectivity values and graph metrics in the beta frequency band.

Keywords Support vector machine · Weighted phase lag index · Functional brain connectivity network · Electroencephalography · Meth dependence

✉ Bahador Makkiabadi
b-makkiabadi@sina.tums.ac.ir

1 Department of Medical Physics and Biomedical Engineering, School of Medicine, Tehran University of Medical Sciences (TUMS), Tehran, Iran

2 Laureate Institute for Brain Research (LIBR), Tulsa, OK, USA

3 Iranian National Center for Addiction Studies (INCAS), Tehran University of Medical Sciences (TUMS), Tehran, Iran

4 Department of Medical Physics and Biomedical Engineering, School of Medicine, Shahid Beheshti University of Medical Sciences (SBMU), Tehran, Iran

5 Iranian Center of Neurological Research, Neuroscience Institute, Tehran University of Medical Sciences (TUMS), Tehran, Iran

6 Research Center for Biomedical Technology and Robotics (RCBTR), Institute of Advanced Medical Technologies (IAMT), Tehran University of Medical Sciences (TUMS), Tehran, Iran

Introduction

Meth is a highly addictive drug that its consumption causes the feeling of awareness, high energy, and exhilaration. These psycho effects, relatively easy access, and cheap price have made it very popular among young adults. World drug reports shows that there are around 14–54 million users of amphetamines worldwide (Hu et al. 2017). Meth abuse is associated with neurotoxicity, cognitive disorders, auditory or visual hallucinations, bizarre beliefs, risky behaviors, and psychological problems (McKetin et al. 2006). Therefore, Meth dependence is a large burden on societies and it is required to increase the knowledge about it in physiological and neurological terms to improve associated diagnosis and treatments. Accordingly, a reliable detection method for differentiating meth dependent individuals (MDIs) from normal controls (NCs) using brain functional connectivity network (FCN) information would be a powerful clinical tool that could guide treatment modifications.

Functional magnetic resonance imaging (fMRI) and EEG have been widely used to acquire knowledge about disorders related to brain malfunction such as depression, schizophrenia, Alzheimer and addiction (Ma et al. 2010; Wetherill et al. 2018). The EEG is a portable setup which is less expensive than fMRI and is recorded by non-invasive electrodes. It has high temporal resolution proper to study electrophysiology of the brain in different frequency bands. To date, several studies have been done to address issues related to screening individuals with substance dependence from healthy controls using resting-state EEG (rEEG) or event related potentials (ERP), such as studies on opiate (e.g. heroin) (Hu et al. 2017), depressant (e.g. alcohol) (Bae et al. 2017; Mumtaz et al. 2017, 2018a, b), and stimulant substances (e.g. cocaine) (Dunning et al. 2011). Most of these studies concentrated on analyzing time series from few specific nodes (EEG electrodes) on the scalp, while whole brain function cannot be efficiently investigated from limited number of nodes. Accordingly, recent researches have focused on EEG data recorded by several electrodes (e.g. 32 or 64 electrode) and computed their relation to differentiate substance users from healthy non-users (Bae et al. 2017; Hu et al. 2017; Mohagheghian et al. 2018; Mumtaz et al. 2018a). Mumtaz et al. (2018a) used an rEEG-based functional connectivity measure to automatic detection of alcohol use disorder and yielded high performance results. Bae et al. (2017) have computed time-domain effective connectivity and graph features using an online ERP database and a machine learning method to distinguish alcoholic subjects from NCs. Similar rEEG connectivity based study also was performed for differentiating between heroin dependent individuals and NCs by developing a PCA based algorithm (Hu et al. 2017). Another study aimed to distinguish MDIs from NCs that employed ERPs elicited by a visual paradigm including drug related and neutral cues (Shahmohammadi et al. 2016). This paradigm raises drug cravings temporarily and needs patient's attention compared to rEEG analysis approach. Therefore, better differentiation can be performed when considering whole brain functional connectivity of rEEG. Accordingly, main objectives of the current research are (1) automatic detection of meth dependence with high accuracy to be helpful as a complementary method along with standard biochemical tests, given many MDIs often deny their addiction and hence use procedures to negate the result of biochemical tests, (2) identification of most discriminative EEG frequency bands according to whole-brain FCN to help better treatment and screening of MDIs in future.

To these ends, FCN of the two recruited groups were constructed by weighted phase lag index (WPLI) in the six frequency bands. Then, significant differences in graph features and also pairwise connectivity values were obtained as follows.

Materials and methods

The current study was conducted according to the block-levels illustrated in Fig. 1. Namely, after selection of eligible subjects, their EEG signals were recorded during eye-open resting state. Next, recorded signals were subject to necessary preprocessing such as filtering and artifact rejection. Then, construction of FCN carried out by proper connectivity index. After that, graph metrics related to brain-network topology were computed and along with pairwise connectivity of brain regions (EEG electrodes) underwent statistical test to select from which the most discriminate features. The discriminative ones were used to training and testing a machine learning model. Finally the findings were discussed according to classifying results and yielded differences between MDIs and NCs. In the following sections, the steps of procedure are explained in details.

Participants

EEG data were recorded from 36 MDIs, who were in abstinent stage, and 24 age-matched NCs. All patients were under a course of abstinence-based therapy in "Peyrovan Hemmat Harm Reduction Institute" and "Iranian National Center for Addiction Studies (INCAS)" located in Tehran. A psychiatrist performed interview sessions to identify patients who had a history of minimum 6 months of methamphetamine use disorder and no current psychiatric disorders based on DSM-5 axis I. Demographic and

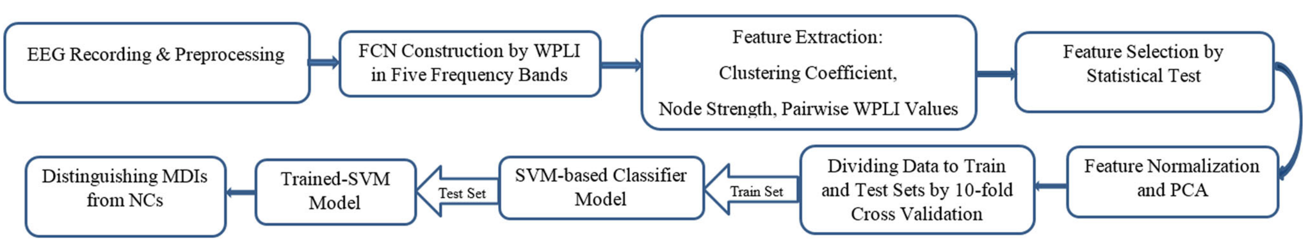

Fig. 1 Block diagram of the proposed system for distinguishing between normal subjects and patients

Table 1 Demographic and substance abuse characteristics

	Descriptive statistics	
	MDIs	NCs
Gender (men)	36/36	24/24
Age	30.55 ± 6.43	30.75 ± 4.63
Education (years)	14.36 ± 2.79	16.58 ± 2.5
Duration of meth abstinence (months)	1–6	–
Duration of meth dependence (years)	8.35 ± 4.07	–
Marital status (married)	36/25	24/7
Number of subjects with a history of opium abuse	36/20	24/0
Number of subjects with a history of alcohol abuse	36/23	24/0
Number of subjects with a history of heroin abuse 30/2	36/5	24/0
Number of subjects with a history of cigarette smoking	36/35	24/2

substance abuse characteristics of the subjects are brought in Table 1.

EEG recording and preprocessing

EEG recording

During EEG recording, all the participants were instructed to see a black color background in the front screen and attempt not to think of anything during EEG recording. The rEEG recorded from MDIs is part of our registered brain stimulation trial in Iranian Registry of Clinical Trials (IRCT) in 2018 with the code IRCT20170808035562N2. All subjects signed a written informed consent form. All the EEG data were recorded using a 62-channel g.tec (http://www.gtec.at/) EEG system (g. HIamp) with sampling rate of 512 Hz at NBML (https://nbml.ir/EN). The electrode placement followed the international 10–10 system and the reference channel was placed on right ear lobe for all individuals. The remained 61 channels were "AFz, Fp1,Fp2, AF3, AF4, F7, Fz, F8, FC5, FC1, FC2, FC6, T7, C3, Cz, C4, T8, CP5, CP1, CP2, CP6, P7, P3, Pz, P4, P8, PO3, PO4, O1, O2, AF7, AF8, F5, F1, F2, F6, FT7, FC3, FCz, FC4, FT8, C5, C1, C2, C6, TP7, CP3, CPz, CP4, TP8, P5, P1, P2, P6, PO7, POz, PO8, Oz, P9, P10, TP9".

EEG pre-processing

EEG data were preprocessed using EEGLAB (Delorme and Makeig 2004) and Fieldtrip (Oostenveld et al. 2011) toolboxes of MATLAB. The datasets were resampled to 200 Hz to decrease computational cost. Then, the data were filtered by a 0.1 Hz high-pass filter to remove the voltage drift and by a notch filter to remove 50 Hz power line noise with its harmonic frequencies. The data were referenced to common average and artifact rejection was firstly performed by visual inspection. Independent component analysis was employed to remove artifactual components (e.g. eye blinks, eye movements, heartbeat, and muscle artifacts). Then, with a moving window and a peak-to-peak threshold all parts exceed ± 75 µv were removed. The preprocessed data, containing the least amount of artifacts, was segmented into 5-s trials(18–24 trials, totally 90–120 s) when the total duration was in the range of previous resting-state studies (Hardmeier et al. 2014; González et al. 2016). Fieldtrip and Brain Connectivity Toolboxes were utilized to connectivity analysis (Rubinov and Sporns 2010).

WPLI computation and FCN construction

Weighted phase lag index description

WPLI is an improved version of PLI connectivity index, proposed by Vinck et al. (2011). This connectivity measure is greatly sensitive and potent to properly detect phase interactions of spatially close signals, offering robustness to volume conduction, so that outperforms PLI, coherence, and imaginary coherence (Vinck et al. 2011; Ewald et al. 2012; Haufe et al. 2013). Characterization of WPLI-based networks, derived from high-resolution EEG, is highly reliable that is important requirement for studies of brain disorders (Hardmeier et al. 2014). WPLI estimates the phase leads and lags between two interacted time-series.

$$WPLI_{xy} = \frac{n^{-1}\sum_{t=1}^{n}\left|imag\left(S_{xyt}\right)\right|\mathrm{sgn}\left(imag\left(S_{xyt}\right)\right)}{n^{-1}\sum_{t=1}^{n}\left|imag\left(S_{xyt}\right)\right|} \quad (1)$$

where S_{xyt} is the cross-spectrum of time-series x and y at time point t, and sgn is the sign function. Function $imag(.)$ returns only the imaginary component of the cross-spectrum. WPLI weights the cross-spectrum according to the imaginary component's magnitude. This allows it to limit the impact of small noise on "true "sgn of cross-spectrum around the real axes.

FCN construction

After applying Laplacian filter to EEG data to reduce volume conduction effect and spatially enhance the data (Hjorth 1975), functional connectivity was computed in EEG-sensor space among pairwise electrodes. The connectivity values were calculated for six frequency bands: delta (1–4 Hz), theta (4–8 Hz), alpha (8–15 Hz), beta (15–30 Hz), gamma (30–45 Hz) and wideband (1–45 Hz) (Hu et al. 2017). Accordingly, we obtained a functional network with 61 nodes in the six bands ($6 \times 61 \times 61$ connectivity matrix) for each subject, where the nodes are the sensors and the link between them are absolute value of the WPLI matrix. The WPLI is highly sensitive to properly detect phase interactions of spatially close signals and shows robustness to volume conduction that outperforms PLI, coherence, and imaginary coherence (Vinck et al. 2011; Ewald et al. 2012; Haufe et al. 2013).

Feature extraction (graph theory-based measures)

It has been shown that node strength and clustering coefficient, two measures from network graph, change in substance dependent individuals (Ahmadlou et al. 2013; Jiang et al. 2013; Wang et al. 2015b). Hence, we considered these two metrics, in combination with pairwise connectivity values, to discriminate MDIs and NCs.

Node strength

The node strength is sum of the weights of links (edges) connected to a node.

$$k_i^w = \sum_{j \in N} w_{ij} \tag{2}$$

where N is the set of all nodes in the network and the links (i, j) are related by connection weight w_{ij}.

Clustering coefficient

The number of weighted triangles around a node i is defined as a basis for measuring segregation:

$$t_i^w = \frac{1}{2} \sum_{j,h \in N} (w_{ij} w_{ih} w_{jh})^{\frac{1}{3}} \tag{3}$$

Clustering coefficient reflects the degree that the connected nodes in a graph tend to form clusters and can illustrate the degree of local connectivity in the network (Watts and Strogatz 1998; Bullmore and Sporns 2009). The clustering coefficient of the network is described by:

$$C^w = \frac{1}{n} \sum_{i \in N} c_i^w = \frac{1}{n} \sum_{i \in N} \frac{2t_i^w}{k_i(k_i - 1)} \tag{4}$$

Feature selection and principal component analysis

The selected graph measures and connectivity values were those with significant differences ($P < 0.05$) between MDIS and NCs. Principal Component analysis (PCA) is a mathematical procedure by which uncorrelated variables are generated form correlated variables. To improve classifier performance, PCA were applied to normalized graph measures and functional connectivity values to provide a feature set with minimum redundancy. Accordingly, a new feature vector was produced by keeping two first PCA components (the first components corresponding to the largest eigenvalues).

Support vector machine (SVM) classifier model

SVM is a supervised classifier that can be applied with several kernels such as linear, polynomial and radial basis function (RBF) kernel (Burges 1998; Alvar et al. 2017). We trained and tested a SVM with RBF to classify individuals with meth dependence from healthy controls. SVM works well with a small number of training samples and a huge number of features (Vapnik 2013). To find a good fit, meaning one with a low cross-validation loss, the Kernel-Scale option (RBF sigma parameter) was set by Bayesian optimization in MATLAB (Snoek et al. 2012). The SVM classifier with RBF kernel was validated using tenfold cross validation for obtaining a robust estimation of the classification performance. All the mentioned processes were separately carried out for each frequency band. The statistical significance of the classification results were evaluated by 5e3 permutation tests by making classifiers on the data when the class labels were randomly assigned (Ojala and Garriga 2010). Furthermore, F-score and area under receiver operating characteristic curves (AUROC) were also computed based on the classification scores of testing subjects (Zweig and Campbell 1993).The classifier has better performance in a frequency band for which the AUROC and F-score are higher than those of the other bands.

Results

Figure 2a, b shows the 61×61 functional connectivity matrices for MDIs and NCs in the six frequency bands. Figure 2c illustrates significant differences in coupling between pairwise electrodes. In this regard, the significance level $\alpha = 0.05$ was selected and false discovery rate (FDR) was performed with $q < 0.05$ to correct for multiple comparisons. There were differences in all the frequency bands except in the alpha band: FT7-P7, Fz-P5, and AF4-OPz in the delta band; T8-CP3, T8-Pz in the theta band; P8-O2, P4-O2, CPz-P3, T8-P9, Cz-TP7and C2-FCz in the beta band; AF8-P5, F8-P8 and FT8-PO8 in the gamma band. Totally, the number of connectivity pairs abnormally changed is greater in the beta oscillatory rhymes compared to the other oscillatory bands. Further, the average values of whole-brain WPLI were significantly increased in MDIs (0.0016 ± 0.0009) compared to that of NCS (0.0011 ± 0.0007) (F = 4.24, $P = 0.043$) in the beta bands (Fig. 3). There were significant differences in graph metrics, node strength and weighted clustering coefficient, at nodal level. The name of these nodes and corresponding P values are brought in Tables 2 and 3.

Table 4 includes classification results for the two study groups involving the MDIs and NCs. As shown in the table, among the EEG frequency bands the delta band revealed best F-score (0.82) using only the significant differences in graph metrics. When the significant differences in pairwise connectivity were used, the best results were obtained in the beta band (F-score = 0.86). Combination of the graph metrics with the connectivity values improved the results, so that the best results were obtained in the beta band (F-score = 0.94, average of AUROC = 0.95).

The result of permutation test indexed that the classification result was more statistically significant for the beta band (P <2e−4) compared to the delta, theta, alpha, gamma and wide bands that respectively yielded $P < 0.001$, $P < 0.04$, $P < 0.4$, $P < 0.1$ and $P < 0.009$ (Fig. 4).

To assess self-reported impulsivity, depression, anxiety and stress, Barratt Impulsiveness Scale-11 (BIS-11) and Depression Anxiety Stress Scale-21 (DASS-21) were used. Table 5 shows the summary results of these scales and their correlation with the whole-brain connectivity (mean WPLI) in the beta frequency band for MDIs and NCs.

The anxiety and stress level of MDIs were significantly greater than those of NCs ($P < 0.001$), but the Pearson correlation results showed no significant correlation between the DASS and BIS subscales and the whole-brain connectivity.

Discussion

In this study, we introduced fundamental changes in the brain functional coupling of MDIs compared to that of NCs. A SVM classifier was successfully designed using the coupling differences and graph metrics of brain FCN to distinguish between the two groups. The changes in graph metrics is intrinsically emerged from the pairwise connectivity differences in the FCN. Hence, we included the connectivity changes as well as the graph metrics as features to SVM. This strategy is helpful in understanding the brain physiological processes in MDIs that can be distinguished from NCs. The results indicated that MDIs had a hypo-connected FCN in the beta frequency band compared to NCs.

EEG activity and impulsiveness, depression, anxiety and stress scales

High level of impulsivity is associated with resting-state EEG in gambling disorder (GD) as a type of addiction. study of Lee et al. (2017) indicated that GD patients with high level of impulsivity (25th percentile of BIS-11 scores) revealed decreased theta absolute power, and decreased alpha and beta absolute power compared to GD patients with middle (26th–74th percentile) and low impulsivity (75th percentile). Accordingly, MDIs, recruited in our study, had either low or middle level of impulsivity. Further, the correlation analysis did not reveal significant relationship between impulsivity components of MDIs and the whole-brain connectivity values in the beta frequency band (Table 5). Jena (2015) reported that baseline EEG in subjects with mild and moderate stress is alpha wave and in whom with high stress is beta wave. Among our recruited subjects, just 8 subjects among MDIs had high stress (see Table 6). Further, the correlation analysis showed that there is not significant relationship between stress, anxiety, depression and the whole-brain connectivity values of MDIs and NCs. Hence, it could be concluded that our observed differences in brain connectivity in the beta frequency band are probably due to methamphetamine dependence and its effect on brain resting-state networks, altered in different substance use disorders (SUDs) (Zilverstand et al. 2018), than due to impulsivity, depression, anxiety and stress.

Beta frequency band alterations in SUDs

Newson and Thiagarajan (2018) carried out a new review on studies of psychiatric disorders that used resting-state EEG to investigate spectral power variation in different frequency bands. They considered three types of addiction: opioids (Wang et al. 2015a; Motlagh et al. 2017; Zhao et al. 2017), alcohol (Günther et al. 1997; Bauer 2001; Rangaswamy et al. 2002, 2003; Saletu-Zyhlarz et al. 2004; Fein and Allen 2005; Son et al. 2015; Herrera-Diaz et al. 2016) and internet (Choi et al. 2013; Son et al. 2015; Kim et al. 2017) which is beside substance addiction disorders according to 11th Revision of the International Classification of Diseases (ICD-11). According to that review, the

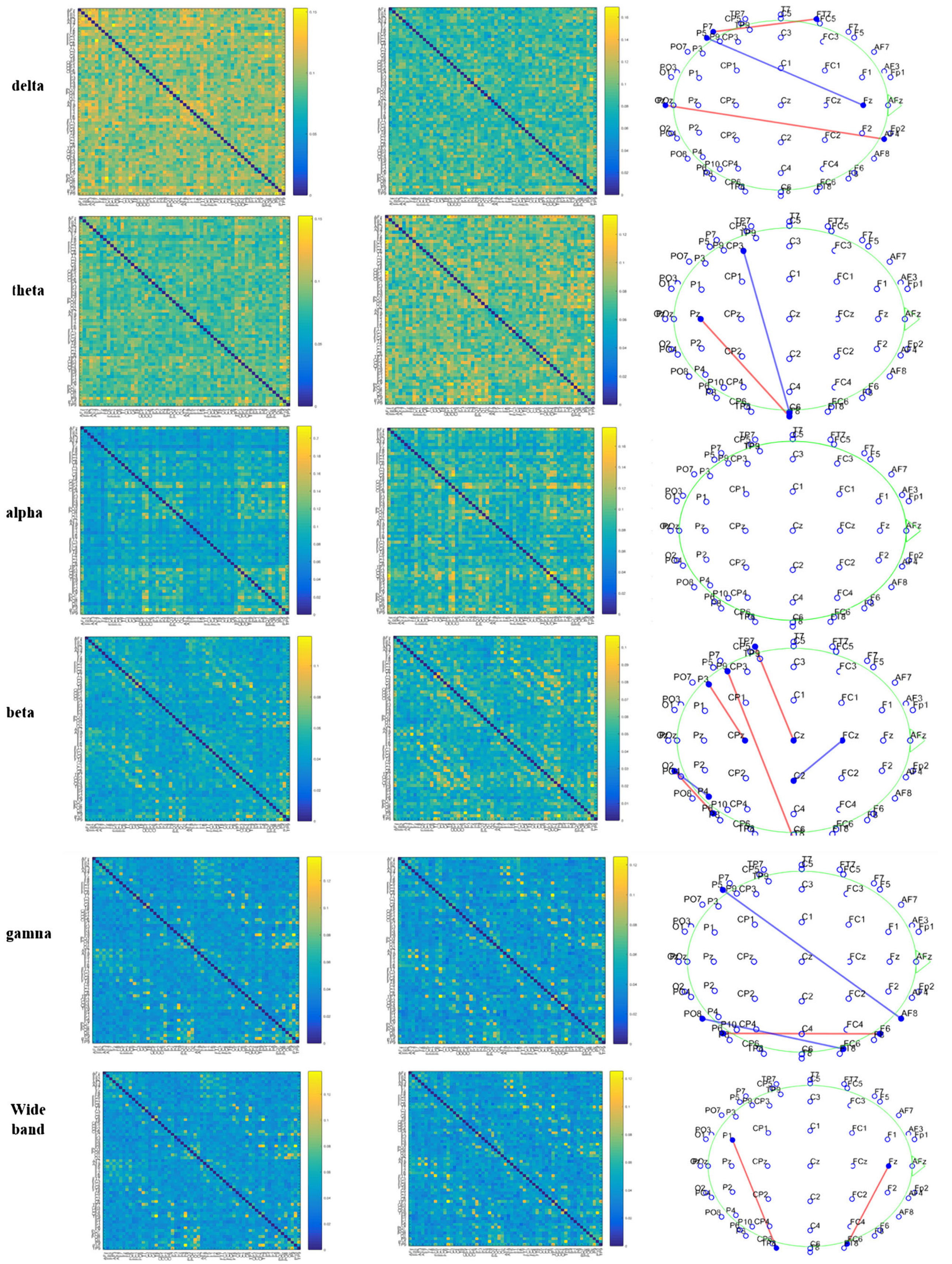
delta
theta
alpha
beta
gamna
Wide band

◀**Fig. 2** Functional connectivity matrixes of MDIs (left column) and NCs (middle column) in the delta, theta, alpha, beta, gamma and wide (1–45 Hz) frequency bands. Significant pairwise connectivity differences after FDR correction on EEG sensor space (right column). Blue color means connectivity value of MDIs > NCs and red means NCs < MDIs

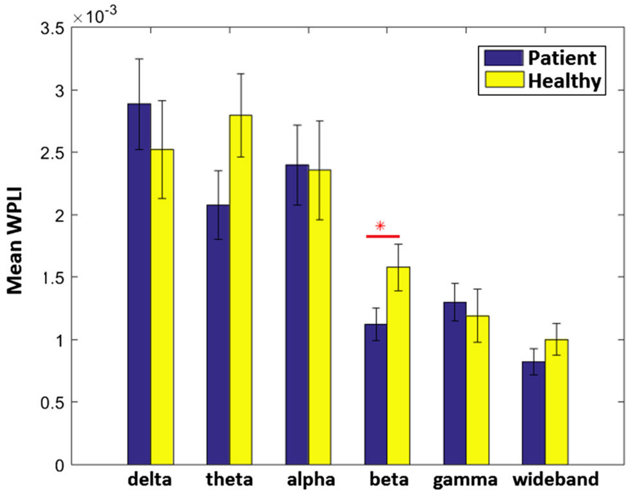

Fig. 3 Bar plot of mean ± SE connectivity values in the six frequency bands. The star flags significance level ($P < 0.05$)

most frequently (dominant) findings (significant increase, significant decrease) across the three types of SUDs are related to the beta band, given the beta power spectrum enhanced for opioid and alcohol users (vs. healthy controls) while attenuated for internet addiction. Regarding the other frequency bands, no dominant results have been reported in these type of SUDs (Newson and Thiagarajan 2018).

Some other researches, not included in the review study of Newson et al. further observed the beta related alterations in SUDs versus controls. Namely, Huang et al. (2018) found that abnormal BOLD signal levels in the dorsal anterior cingulate cortex (dACC), nucleus accumbens (NAcc), posterior cingulate cortex (PCC) of alcoholics, caused by arisen craving in a cue-reactivity fMRI experiment, are consistent with increased beta-band activity in the dACC and pgACC in resting-state EEG. Herning et al. (2008) compared 75 marijuana abusers with 33 controls and found relationship between the duration of use and attenuation in alpha and beta power at posterior electrode sites. Polunina and Davydov (2004) conducted a study among 33 heroin-dependent individuals, who were in 6–135 abstinent days, and 13 nonusers. The results revealed enhanced power in the beta rhythms coupled with decreased power in theta, and alpha frequency bands.

Table 2 Nodes (sensors) for which node strength values are significantly different in MDIs compared to NCs

Delta	Fp1/0.03	AF4/0.03	F7/0.0005	FC5/0.03	FC1/0.005	FC2/0.01	TP9/0.02
	6.05 (2)/5.04 (0.82)	6.25 (2.52)/5.25 (1.07)	6.22 (2.28)/4.85 (0.94)	6.37 (2.12)/5.23 (0.97)	5.48 (0.79)/4.89 (0.68)	5.79 (1.57)/4.97 (0.87)	6.26 (2.04)/5.18 (0.90)
	FC6/0.03	T7/0.01	C4/0.001	P4/0.003	PO4/0.008	O1/0.02	FC4/0.04
	5.84 (1.71)/4.95 (0.81)	6.35 (1.63)/5.39 (0.92)	6.19 (1.72)/5.02 (0.76)	5.80 (0.98)/5.08 (0.71)	6.19 (1.79)/5.36 (0.95)	5.82 (1.20)/5.14 (0.91)	6.03 (1.71)/5.16 (1.12)
	F5/0.03	F2/0.008	F6/0.030	FT7/0.001	FC3/0.004		
	5.97 (2.13)/5.03 (0.96)	5.82 (1.67)/4.88 (0.70)	6.07 (1.91)/5.22 (0.75)	6.44 (1.52)/5.27 (0.87)	5.89 (1.57)/4.82 (0.96)		
Theta	AF4/0.02	F8/0.03	CP6/0.03	AF8/0.0005	TP9/0.008		
	5.28 (1.34)/4.58 (1.05)	4.77 (1.2)/4.19 (0.75)	5.01 (1.14)/4.51 (1.12)	5.00 (1.13)/4.07 (0.59)	5.1437 (1.20)/ 4.53 (1.09)		
Alpha	P6/0.03						
	5.72 (2.17)/4.71 (1.45)						
Beta	CP2/0.03	P6/0.003	POz/0.02				
	2.74 (0.73)/3.07 (0.83)	2.93 (0.67)/2.44 (0.57)	2.70 (0.65)/3.12 (0.80)				
Gamma	Fp2/0.03	F8/0.03	T8/0.01	CP2/0.01	AF8/0.01		
	2.79 (0.60)/2.47 (0.53)	2.84 (0.71)/2.62 (0.98)	3.25 (0.96)/2.91 (1.11)	2.72 (0.57)/2.38 (0.61)	2.92 (0.67)/2.60 (0.71)		
Wide band	F8/0.03						
	1.96 (0.49)/1.73 (0.53)						

Node name/P value; mean (SD) of MDIs/mean (SD) of NCs

Table 3 Nodes (sensors) for which clustering coefficient values are significantly different in MDIs compared to NCs

Delta	F7/0.0005	T7/0.01	C3/0.05	C4/0.001	FC3/0.004	TP9/0.02
	0.18 (0.02)/0.16 (0.02)	0.19 (0.02)/0.17 (0.02)	0.18 (0.02)/0.17 (0.02)	0.19 (0.03)/0.17 (0.02)	0.18 (0.02)/0.16 (0.03)	0.19 (0.03)/0.17 (0.02)
Theta	AF8/0.0005	TP9/0.008				
	0.18 (0.03)/0.16 (0.02)	0.18 (0.02)/0.16 (0.02)				
Alpha	Fp2/0.07	C4/0.24				
	0.15 (0.03)/0.18 (0.03)	0.17 (0.04)/0.19 (0.03)				

Node name/*P* value; mean (SD) of MDIs/mean (SD) of NCs

Table 4 Statistical results of SVM classifier to distinguish MDIs from NCs

Features	Frequency band	Sigma of RBF	Accuracy (%)	Sensitivity (%)	Specificity (%)	F-score	AUROC
Graph features	Delta	0.181	76	94	50	0.82	0.70 ± 0.1
	Theta	0.086	66	86	37	0.75	0.62 ± 0.17
	Alpha	0.069	56	80	20	0.69	0.36 ± 0.08
	Beta	0.063	61	83	29	0.72	0.48 ± 0.1
	Gamma	0.070	93	77	25	0.68	0.52 ± 0.13
	Wideband	0.07	50	75	12	0.64	0.39 ± 0.29
Pairwise connectivity values	Delta	0.079	73	83	58	0.78	0.69 ± 0.12
	Theta	0.045	65	86	33	0.74	0.55 ± 0.09
	Alpha	0.069	56	80	20	0.69	–
	Beta	0.241	83	88	75	0.86	0.82 ± 0.17
	Gamma	0.083	68	75	58	0.73	0.76 ± 0.12
	Wideband	0.09	58	83	20	0.7	0.65 ± 0.69
Integration of graph features and connectivity values	Delta	0.191	76	88	58	0.82	0.82 ± 0.16
	Theta	0.090	71	80	58	0.77	0.63 ± 0.27
	Alpha	0.068	63	86	29	0.73	0.46 ± 0.15
	Beta	**0.306**	**93**	**100**	**83**	**0.94**	**0.95 ± 0.06**
	Gamma	0.083	66	83	41	0.75	0.53 ± 0.29
	Wideband	0.1	66	77	50	0.73	0.73 ± 0.1
Integration of graph features and connectivity values of all the bands		0.35	93	94	91	0.94	0.96 ± 0.08

The AUROC is computed for tenfold (Mean ± SD)

The best results, which are related to the beta frequency band, are bold

Another study conducted by Franken et al. (2004) also reported increased beta power in smaller number of heroin patients (14 days of abstinence). Further, Fingelkurts et al. (2006) reported that opioid dependence results in increased local and decreased remote functional connectivity in the alpha and beta frequency bands. Also, in the current study, decreased beta band connectivity occurred in MDIs at central-parietal and temporal-parietal regions. The correlation results indicate that abnormal whole-brain FCN in this frequency band is not related to impulsivity, stress and depression (Table 5). The connectivity differences in the beta frequency band caused higher classifier performance (F-score = 0.86) compared to the other bands, which might be another evidence of distinguished abnormal function of the brain in this specific frequency band for MDIs.

In sum, However, the number of studies among SUDs that converged on being abnormality in the beta band is not yet considerably high, and there is high methodological variability in them (functional connectivity and power spectrum analysis with eye-close/eye-open resting-state EEG), compared with the other frequency bands the beta band encompasses more significant differences of SUDs

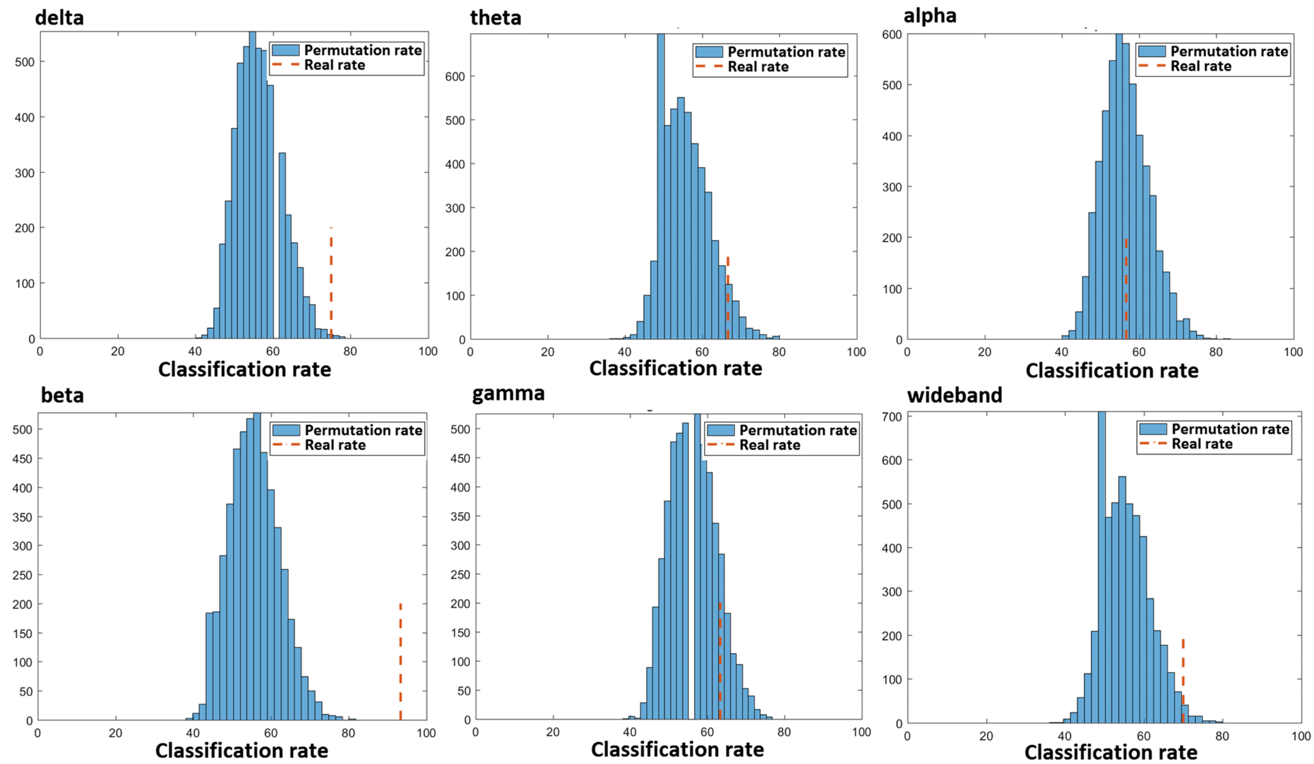

Fig. 4 The permutation classification rates of 5e3 permutation tests and real classification rates of the cross-validation results in the six frequency bands

Table 5 Results of correlations between anxiety, depression, stress and impulsivity and the average values of whole-brain WPLI in the beta band for the patient group

Characteristic	# (MDIs/NCS)	Mean (SD)		t	P value	Pearson corr. coef./P value	
		MDIs	NCs			MDIs	NCs
Stress	30/21	19.66 (10.62)	6.10 (2.7)	6.4	< 0.001	0.080/0.67	0.27/0.22
Anxiety	31/23	12.90 (8.66)	5.5 (5.6)	3.7	< 0.001	− 0.039/0.83	− 0.07/0.74
Depression	29/23	18.34 (10.14)	14.2 (6.4)	1.7	0.08	− 0.045/0.81	0.14/0.49
Attention impulsivity	36/–	12.11 (4.81)				− 0.123/0.47	
Motor impulsivity	33/–	15.3 (6.17)				− 0.120/0.50	
Nonplanning impulsivity	35/–	17.62 (4.09)				− 0.010/0.95	

versus healthy controls. Accordingly, it could be concatenated that the beta band has more potential to be a biomarker for SUDs compared to the other frequency bands and it may be associated with inhibitory deficits in SUDs.

Comparing with previous studies

There are many studies, mostly among alcoholics, that used knowledge-based systems based on EEG signals to support human decision-making to predict substance dependence and also to produce knowledge for developing related treatments to quite substance abuse. Table 7 includes the newest studies that aimed to detect meth abuse or to detect other type of substance abuse while used EEG and functional connectivity in their approach.

Shahmohammadi et al. (2016) have performed the first ERP-based study to distinguish ten meth abusers from ten normal controls using 32 channels EEG. They used area under windowed ERPs elicited by a visual paradigm including drug related and neutral images to distinguish MDIs and NCs that yielded 80% accuracy without reporting sensitivity and specificity. Ahmadlou et al. (2013) Have investigated functional brain organization of 36 meth abusers by rEEG recorded from 32 scalp

Table 6 Number of subjects in different stress, anxiety, and depression levels

	Normal	Mild	Moderate	High	Sever
MDIs					
Stress	12	2	8	3	5
Anxiety	9	3	8	4	7
Depression	5	6	7	4	7
NCs					
Stress	21	0	–	–	–
Anxiety	16	4	1	1	1
Depression	3	8	10	0	2

electrodes and reported disrupted functional connectivity in the gamma band. They considered the frequency range of 30–60 Hz for the gamma band that is influenced by 50 Hz notch filtering effect. We primarily used this range of frequency for the gamma band and found significantly increased whole-brain clustering coefficient in MDIs compared to NCs. Thus, we limited this frequency range to 30–45 Hz to eliminate filtering effect on connectivity values by following other studies (Hu et al. 2017; Park et al. 2017). The gamma band FCN differences between MDIs and NCs, reported by a similar study (Ahmadlou et al. 2013), may be related to abstinent duration and withdrawal effect rather than the meth abuse effect. This speculation raised from the fact that our subjects were in short term abstinent stage (1–6 months) without correlated results of self-reported emotional questioners with whole-brain connectivity in their distinctive frequency band, i.e. beta band, while that of (Ahmadlou et al. 2013) were in early abstinent stage (1–3 weeks) with correlated results of the self-reported emotional questioners with the brain-topology in their distinctive frequency band, i.e. gamma band. This will be more investigated by EEG source reconstruction methods in our future studies. Considering the recruitment of MDIs with long-term abstinent stage, having fewer withdrawal symptoms, would be recommended to future studies to investigate the mentioned speculation.

Connectivity based classification was recently studied among alcoholism by ERP (Bae et al. 2017) or rEEG (Mumtaz et al. 2017). In Study of Mumtaz et al. (2017), inter-hemispheric coherences and spectral power for EEG delta, theta, alpha, beta and gamma were integrated resulted in F-score = 0.9. Study of Bae et al. (2017) constructed effective whole brain-connectivity network using Granger causality and graph metrics extracted from an existing ERP dataset resulted the classification accuracy of 90%, sensitivity of 95.3%, and specificity of 82.4%. These results shows that extracted features from whole brain network compared to regional-based analysis is more efficient in differentiating different type of substance abusers from healthy controls. Many MDIs try to use strategies to negatively affect the biochemical test of their addiction. Therefore, the use of additional analysis-based techniques along with the biochemical test can result in more reliable diagnosis. Utilizing rEEG to differentiate substance

Table 7 Related studies about EEG application to distinguish substance dependent individuals from healthy controls

Study	Patients/controls	Data type/electrodes	Substance	Method	F-score/accuracy (%)
Mumtaz et al. (2018a, b)	30/30	rEEG/19	Alcohol	Synchronization-likelihood features with different classifiers (SVM, Naïve Bayesian, and Logistic Regression)	0.97/0.98
Mumtaz et al. (2017)	30/15	rEEG/19	Alcohol	Spectral powers of different bands and inter-hemispheric coherences with logistic regression classifier	0.89/87
Bae et al. (2017)	37/23	ERP/61	Alcohol	Significant nodal-gragh features of directional FCN with SVM classifier	–/90
Hu et al. (2017)	15/14	rEEG/64	Heroin	directional FCN constructed by independent component analysis for blind source decomposition	–
Ahmadlou et al. (2013)	36/36	rEEG/32	MA	Average of graph features of whole-brain FCN and EPNN classifier	–/82.8
Shahmohammadi et al. (2016)	10/10	ERP/32	MA	The area of positive sections below each windowed ERP	–
The current study	36/24	rEEG/61	MA	Integrated pairwise WPLI values and nodal-graph features of FCN with SVM classifier	0.94/0.93

MA = meth

dependent individuals is potentially robust to denial attempts and hence could be helpful in distinguishing denying addicted subjects. The connectivity based differentiation could also be helpful for investigating the effectiveness of treatment as well as predicting of possible relapse.

There are also some limitations in this study. First, only male subjects were recruited, while gender can influence the vulnerability to meth toxicity. Second, due to practical difficulties in recruitment of MDIs the sample size (36 MDIs) was moderate. Third, the demographical and behavioral matching was not done because of intrinsic limitations.

Conclusion

Our results show that the beta band waves are abnormally changed in MDIs versus normal controls. Moreover, the proposed feature vectors, including brain FCN node strength and pairwise functional connectivity values in the beta band, are great metrics to differentiate MDIs from NCs. Accordingly, the beta band related information might be useful for evaluating efficacy of treatments for MDIs.

Acknowledgements The authors wish to thank TUMS and CSTC for financial support of this research and also National Brain Mapping Laboratory (NBML) for their instrumental support.

Funding This work was supported in part by Tehran University of Medical Sciences (TUMS) (https://www.tums.ac.ir/?lang=en), project Grant No. of 95-02-30-32441, and also by Cognitive Sciences and Technologies Council (CSTC) (http://cogc.ir/?lang=2) Grant No. of 4517. The funders has played no role in the research. The funders had no role in study design, data collection and analysis, decision to publish, or preparation of the manuscript.

Compliance with ethical standards

Conflict of interest The authors declare that they have no conflict of interest.

Ethical approval The experimental was reviewed and approved by the ethics committee of Tehran University of Medical Sciences (Iran) (Ethical Committee Approval Code: IR.TUMS.MEDICINE.REC.1395.1621).

References

Ahmadlou M, Ahmadi K, Rezazade M, Azad-Marzabadi E (2013) Global organization of functional brain connectivity in methamphetamine abusers. Clin Neurophysiol 124(6):1122–1131

Alvar AA, Deevband MR, Ashtiyani M (2017) Neutron spectrum unfolding using radial basis function neural networks. Appl Radiat Isot 129:35–41

Bae Y, Yoo BW, Lee JC, Kim HC (2017) Automated network analysis to measure brain effective connectivity estimated from EEG data of patients with alcoholism. Physiol Meas 38(5):759

Bauer LO (2001) Predicting relapse to alcohol and drug abuse via quantitative electroencephalography. Neuropsychopharmacology 25(3):332–340

Bullmore E, Sporns O (2009) Complex brain networks: graph theoretical analysis of structural and functional systems. Nat Rev Neurosci 10(3):186

Burges CJ (1998) A tutorial on support vector machines for pattern recognition. Data Min Knowl Discov 2(2):121–167

Choi JS, Park SM, Lee J, Hwang JY, Jung HY, Choi SW, Kim DJ, Oh S, Lee JY (2013) Resting-state beta and gamma activity in Internet addiction. Int J Psychophysiol 89(3):328–333

Delorme A, Makeig S (2004) EEGLAB: an open source toolbox for analysis of single-trial EEG dynamics including independent component analysis. J Neurosci Methods 134(1):9–21

Dunning JP, Parvaz MA, Hajcak G, Maloney T, Alia-Klein N, Woicik PA, Telang F, Wang GJ, Volkow ND, Goldstein RZ (2011) Motivated attention to cocaine and emotional cues in abstinent and current cocaine users—an ERP study. Eur J Neurosci 33(9):1716–1723

Ewald A, Aristei S, Nolte G, Rahman RA (2012) Brain oscillations and functional connectivity during overt language production. Front Psychol 3:166

Fein G, Allen J (2005) EEG spectral changes in treatment-naive, actively drinking alcoholics. Alcohol Clin Exp Res 29(4):538–546

Fingelkurts AA, Fingelkurts AA, Kivisaari R, Autti T, Borisov S, Puuskari V, Jokela O, Kahkonen S (2006) Increased local and decreased remote functional connectivity at EEG alpha and beta frequency bands in opioid-dependent patients. Psychopharmacology 188(1):42–52

Franken IH, Stam CJ, Hendriks VM, van den Brink W (2004) Electroencephalographic power and coherence analyses suggest altered brain function in abstinent male heroin-dependent patients. Neuropsychobiology 49(2):105–110

González GF, Van der Molen M, Žarić G, Bonte M, Tijms J, Blomert L, Stam C, Van der Molen M (2016) Graph analysis of EEG resting state functional networks in dyslexic readers. Clin Neurophysiol 127(9):3165–3175

Günther W, Müller N, Knesewitsch P, Haag C, Trapp W, Banquet J-P, Stieg C, Alper KR (1997) Functional EEG mapping and SPECT in detoxified male alcoholics. Eur Arch Psychiatry Clin Neurosci 247(3):128–136

Hardmeier M, Hatz F, Bousleiman H, Schindler C, Stam CJ, Fuhr P (2014) Reproducibility of functional connectivity and graph measures based on the phase lag index (PLI) and weighted phase lag index (wPLI) derived from high resolution EEG. PLoS ONE 9(10):e108648

Haufe S, Nikulin VV, Müller K-R, Nolte G (2013) A critical assessment of connectivity measures for EEG data: a simulation study. Neuroimage 64:120–133

Herning RI, Better W, Cadet JL (2008) EEG of chronic marijuana users during abstinence: relationship to years of marijuana use, cerebral blood flow and thyroid function. Clin Neurophysiol 119(2):321–331

Herrera-Diaz A, Mendoza-Quinones R, Melie-Garcia L, Martinez-Montes E, Sanabria-Diaz G, Romero-Quintana Y, Salazar-Guerra I, Carballoso-Acosta M, Caballero-Moreno A (2016) Functional connectivity and quantitative EEG in women with alcohol use disorders: a resting-state study. Brain Topogr 29(3):368–381

Hjorth B (1975) An on-line transformation of EEG scalp potentials into orthogonal source derivations. Electroencephalogr Clin Neurophysiol 39(5):526–530

Hu B, Dong Q, Hao Y, Zhao Q, Shen J, Zheng F (2017) Effective brain network analysis with resting-state EEG data: a comparison between heroin abstinent and non-addicted subjects. J Neural Eng 14(4):046002

Huang Y, Mohan A, De Ridder D, Sunaert S, Vanneste S (2018) The neural correlates of the unified percept of alcohol-related craving: a fMRI and EEG study. Sci Rep 8(1):923

Jena SK (2015) Examination stress and its effect on EEG. Int J Med Sci Public Health 11(4):1493–1497

Jiang G, Wen X, Qiu Y, Zhang R, Wang J, Li M, Ma X, Tian J, Huang R (2013) Disrupted topological organization in whole-brain functional networks of heroin-dependent individuals: a resting-state FMRI study. PLoS ONE 8(12):e82715

Kim YJ, Lee JY, Oh S, Park M, Jung HY, Sohn BK, Choi SW, Kim DJ, Choi JS (2017) Associations between prospective symptom changes and slow-wave activity in patients with Internet gaming disorder: a resting-state EEG study. Medicine 96(8):e6178

Lee JY, Park SM, Kim YJ, Kim DJ, Choi S-W, Kwon JS, Choi J-S (2017) Resting-state EEG activity related to impulsivity in gambling disorder. J Behav Addict 6(3):387–395

Ma N, Liu Y, Li N, Wang C-X, Zhang H, Jiang X-F, Xu H-S, Fu X-M, Hu X, Zhang D-R (2010) Addiction related alteration in resting-state brain connectivity. Neuroimage 49(1):738–744

McKetin R, McLaren J, Lubman DI, Hides L (2006) The prevalence of psychotic symptoms among methamphetamine users. Addiction 101(10):1473–1478

Mohagheghian F, Makkiabadi B, Jalilvand H, Khajehpoor H, Samadzadehaghdam N, Eqlimi E, Deevband M (2018) Computer-aided tinnitus detection based on brain network analysis of EEG functional connectivity. J Biomed Phys Eng

Motlagh F, Ibrahim F, Rashid R, Seghatoleslam T, Habil H (2017) Investigation of brain electrophysiological properties among heroin addicts: quantitative EEG and event-related potentials. J Neurosci Res 95(8):1633–1646

Mumtaz W, Vuong PL, Xia L, Malik AS, Rashid RBA (2017) An EEG-based machine learning method to screen alcohol use disorder. Cogn Neurodyn 11(2):161–171

Mumtaz W, Kamel N, Ali SSA, Malik AS (2018a) An EEG-based functional connectivity measure for automatic detection of alcohol use disorder. Artif Intell Med 84:79–89

Mumtaz W, Vuong PL, Malik AS, Rashid RBA (2018b) A review on EEG-based methods for screening and diagnosing alcohol use disorder. Cogn Neurodyn 12(2):141–156

Newson JJ, Thiagarajan TC (2018) EEG frequency bands in psychiatric disorders: a review of resting state studies. Front Hum Neurosci 12:521

Ojala M, Garriga GC (2010) Permutation tests for studying classifier performance. J Mach Learn Res 11(Jun):1833–1863

Oostenveld R, Fries P, Maris E, Schoffelen J-M (2011) FieldTrip: open source software for advanced analysis of MEG, EEG, and invasive electrophysiological data. Comput Intell Neurosci 2011:1

Park SM, Lee JY, Kim YJ, Lee JY, Jung HY, Sohn BK, Kim DJ, Choi JS (2017) Neural connectivity in Internet gaming disorder and alcohol use disorder: a resting-state EEG coherence study. Sci Rep 7(1):1333

Polunina AG, Davydov DM (2004) EEG spectral power and mean frequencies in early heroin abstinence. Prog Neuropsychopharmacol Biol Psychiatry 28(1):73–82

Rangaswamy M, Porjesz B, Chorlian DB, Wang K, Jones KA, Bauer LO, Rohrbaugh J, O'connor SJ, Kuperman S, Reich T (2002) Beta power in the EEG of alcoholics. Biol Psychiat 52(8):831–842

Rangaswamy M, Porjesz B, Chorlian DB, Choi K, Jones KA, Wang K, Rohrbaugh J, O'Connor S, Kuperman S, Reich T (2003) Theta power in the EEG of alcoholics. Alcohol Clin Exp Res 27(4):607–615

Rubinov M, Sporns O (2010) Complex network measures of brain connectivity: uses and interpretations. Neuroimage 52(3):1059–1069

Saletu-Zyhlarz GM, Arnold O, Anderer P, Oberndorfer S, Walter H, Lesch OM, Böning J, Saletu B (2004) Differences in brain function between relapsing and abstaining alcohol-dependent patients, evaluated by EEG mapping. Alcohol Alcohol 39(3):233–240

Shahmohammadi F, Golesorkhi M, Kashani MMR, Sangi M, Yoonessi A, Yoonessi A (2016) Neural correlates of craving in methamphetamine abuse. Basic Clin Neurosci 7(3):221

Snoek J, Larochelle H, Adams RP (2012) Practical bayesian optimization of machine learning algorithms. Adv Neural Inf Process Syst 5(1):2951–2959

Son KL, Choi JS, Lee J, Park SM, Lim JA, Lee JY, Kim SN, Oh S, Kim DJ, Kwon JS (2015) Neurophysiological features of Internet gaming disorder and alcohol use disorder: a resting-state EEG study. Transl Psychiatry 5:e628

Vapnik V (2013) The nature of statistical learning theory. Springer, Berlin

Vinck M, Oostenveld R, Van Wingerden M, Battaglia F, Pennartz CM (2011) An improved index of phase-synchronization for electrophysiological data in the presence of volume-conduction, noise and sample-size bias. Neuroimage 55(4):1548–1565

Wang GY, Kydd R, Wouldes TA, Jensen M, Russell BR (2015a) Changes in resting EEG following methadone treatment in opiate addicts. Clin Neurophysiol 126(5):943–950

Wang Z, Suh J, Li Z, Li Y, Franklin T, O'Brien C, Childress AR (2015b) A hyper-connected but less efficient small-world network in the substance-dependent brain. Drug Alcohol Depend 152:102–108

Watts DJ, Strogatz SH (1998) Collective dynamics of 'small-world'networks. Nature 393(6684):440

Wetherill RR, Rao H, Hager N, Wang J, Franklin TR, Fan Y (2018) Classifying and characterizing nicotine use disorder with high accuracy using machine learning and resting-state fMRI. Addict Biol 24(4):811–821

Zhao Q, Jiang H, Hu B, Li Y, Zhong N, Li M, Lin W, Liu Q (2017) Nonlinear dynamic complexity and sources of resting-state eeg in abstinent heroin addicts. IEEE Trans Nanobiosci 16(5):349–355

Zilverstand A, Huang AS, Alia-Klein N, Goldstein RZ (2018) Neuroimaging impaired response inhibition and salience attribution in human drug addiction: a systematic review. Neuron 98(5):886–903

Zweig MH, Campbell G (1993) Receiver-operating characteristic (ROC) plots: a fundamental evaluation tool in clinical medicine. Clin Chem 39(4):561–577